Spatial Sampling for Alignment of Robot Demonstrated Trajectories in Upper Limb Rehabilitation Tasks

Giovanni Braglia
Department of Engineering "Enzo Ferrari"
University of Modena and Reggio Emilia, Modena (Italy)
giovanni.braglia@unimore.it

Dario Onfiani
Department of Engineering "Enzo Ferrari"
University of Modena and Reggio Emilia, Modena (Italy)
dario.onfiani@unimore.it

Davide Tebaldi
Department of Engineering "Enzo Ferrari"
University of Modena and Reggio Emilia, Modena (Italy)
davide.tebaldi@unimore.it

André Eugenio Lazzaretti
Department of Electronics Engineering and Computer Science
Federal Technological University of Paranà, Curitiba (Brazil)
lazzaretti@utfpr.edu.br

Luigi Biagiotti
Department of Engineering "Enzo Ferrari"
University of Modena and Reggio Emilia, Modena (Italy)
luigi.biagiotti@unimore.it

Abstract: In robotics, Learning by Demonstration (LbD) aims to transfer skills to robots by leveraging multiple demonstrations of the same task. These demonstrations are stored in a library and processed to extract a consistent skill representation, typically requiring temporal alignment using techniques like Dynamic Time Warping (DTW). In this article, we propose a novel Spatial Sampling algorithm (SSA) tailored for robot trajectories, which enables time-agnostic alignment by providing an arc-length parametrization of the input trajectories. This method eliminates the need for temporal alignment and enhances skill representation. We demonstrate the effectiveness of SSA in an upper-limb rehabilitation case study, introducing a new human-robot interaction architecture.

Keywords: Human-Robot Interaction, Motion Planning, Space-Time Analysis

1 Introduction

Robot Learning by Demonstration (LbD) aims to teach robots tasks through a small number of demonstrations, making skill transfer intuitive, minimizing data requirements, and

8th Conference on Robot Learning (CoRL 2024), Munich, Germany.

enabling non-experts to work with robots [1]. In LbD architectures, the initial step is analyzing the demonstration set to extract the most informative content, often referred to as the *skill* [2]. This skill is then transferred to the robot, which uses a controller to adapt to its environment and handle internal or external constraints [3]. Before computing skills offline and sending commands to the robot, demonstrations are typically pre-processed to align signals. A key step involves measuring similarity or variance across the demonstrations to extract the skill [4]. However, temporal misalignments often distort comparisons, as timing can introduce inaccuracies in aligning time series. Techniques like Dynamic Time Warping (DTW) are commonly used to measure similarity regardless of timing, though DTW does not fully decouple time for many robotics applications [5, 6].
Once the trajectories are aligned, barycenter computation techniques are typically used to identify the most representative skill from the dataset of demonstrations. Initially, the term barycenter referred to an average sequence that minimizes the squared distance to all series in the demonstration library [7]. In robotics, this is commonly done using Gaussian Mixture Regression (GMR), applied to a Gaussian Mixture Model (GMM) fitted on the DTW-aligned trajectories [4, 8, 9].

We propose a novel architecture that still computes the barycenter using GMM/GMR but aligns the dataset trajectories with a method called Spatial Sampling algorithm (SSA). The SSA filters the input trajectory at evenly spaced points, capturing only its geometric information, independent of the timing variations introduced during the demonstration phase [10, 11]. We validated the proposed algorithm in an upper-limb rehabilitation task. In this setup, an expert (e.g. the therapist) teaches a target exercise to an end-user (e.g. the patient). During the demonstration, the end-user holds the robot's end-effector while the expert guides them through the correct execution. The teaching phase may involve multiple demonstrations with varying timing due to different speed profiles or pauses. In this application, we demonstrate that the proposed SSA/GMR architecture offers three key advantages: (i) it aligns the trajectories in the demonstration dataset to extract the corresponding skill; (ii) it parameterizes the obtained barycenter based on its arc-length domain, allowing any timing law to be applied later; and (iii) it provides a reference path (the barycenter) with well-defined derivatives, facilitating the design of a custom phase-law suited for human-robot interaction.

2 Methodology

2.1 Spatial Sampling

The proposed Spatial Sampling algorithm (SSA) generates a filtered trajectory $\hat{\boldsymbol{y}}(\boldsymbol{s}_k)$, which is a function of the arc-length parameter $\boldsymbol{s}_k$, starting from the demonstrated Euclidean trajectory $\boldsymbol{y}(t)$. The proposed algorithm works as follows. 1) Starting from the sequence of samples $\boldsymbol{y}_{T,i} = \boldsymbol{y}(t_{T,i}) = \boldsymbol{y}(iT)$ for $i \in \{0, \dots, n\}$, obtained by sampling the trajectory $\boldsymbol{y}(t)$ with sampling time T, a linearly interpolating continuous-time function $\boldsymbol{y}_L(t)$ is built. 2) A new sequence $\hat{\boldsymbol{y}}_k$ is created by imposing that $\hat{\boldsymbol{y}}_0 = \boldsymbol{y}_L(0)$ and $\hat{\boldsymbol{y}}_k = \boldsymbol{y}_L(t_k)$ for $k > 0$, where t_k is the time instant that guarantees the following condition:

$$\|\hat{\boldsymbol{y}}_k - \hat{\boldsymbol{y}}_{k-1}\| = \delta, \quad \text{for} \quad k = 1, \dots, m. \tag{1}$$

The parameter δ defines the geometric distance between consecutive samples of the filtered trajectory, and can be freely chosen. The condition (1) implies that the total distance between the first point $\hat{\boldsymbol{y}}_0$ and the generic k-th point $\hat{\boldsymbol{y}}_k$ is given by $k\delta$, which approximates the length of the curve $\boldsymbol{y}_L(t)$ at the time instant t_k with a precision that increases as δ decreases. Therefore, for δ sufficiently small, the spatial sampling algorithm introduces the following mapping between the length $s_k = k\delta$ and the position along the approximating linear curve $\boldsymbol{y}_L$:

$$\hat{\boldsymbol{y}}_k = \boldsymbol{y}_L(t_k), \quad \text{with} \quad t_k = \gamma^{-1}(s_k), \tag{2}$$

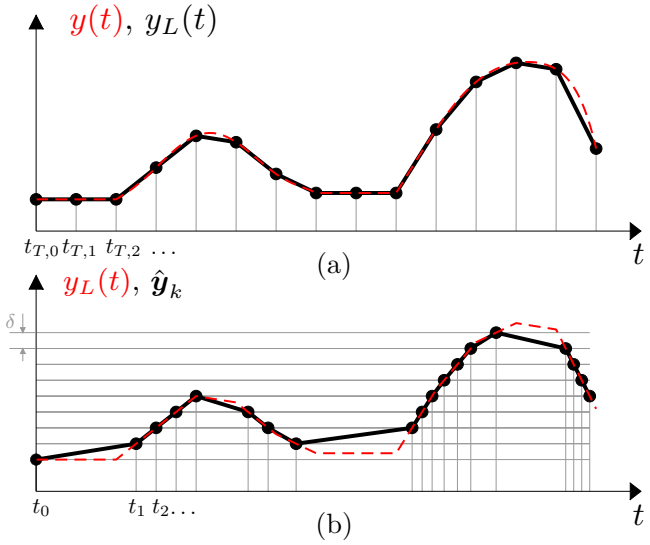

Figure 1: Sketch displaying the operation of the SSA in a one-dimensional scenario. (a) Reference trajectory $\boldsymbol{y}(t)$ sampled with constant period T and interpolating linear curve $y_L(t)$. (b) Sequence of δ-spatially sampled points $\hat{\boldsymbol{y}}_k = \boldsymbol{y}_L(t_k)$.

where $s(t) = \gamma(t)$ is the particular timing law imposed during the trajectory demonstration, describing how the robot moves along the imposed geometric path. Given an analytical approximation $\boldsymbol{\varphi}(s) \approx \hat{\boldsymbol{y}}_k$ the following property holds:

$$\left\| \frac{d\boldsymbol{\varphi}(s)}{ds} \right\|_{s=s_k} \approx \frac{\|\hat{\boldsymbol{y}}_{k+1} - \hat{\boldsymbol{y}}_k\|}{\|s_{k+1} - s_k\|} = \frac{\delta}{\delta} = 1. \tag{3}$$

Consequently the obtained filtered trajectory is a regular curve, given that the derivative in (3) will always be different from zero, and the tangential direction of the curve will always be well-defined. Note that this is of fundamental importance, as it allows any phase velocity profile to be applied later on the curve $\boldsymbol{\varphi}(s)$. Indeed, we can express the velocity of a moving point along the curve as $\dot{\boldsymbol{\varphi}}(s(t)) = \boldsymbol{\varphi}'(s(t))\dot{s}(t)$, with $d\boldsymbol{\varphi}(s)/ds = \boldsymbol{\varphi}'(s)$. Given a desired velocity profile $\dot{\boldsymbol{\varphi}}^\star(t)$, one can straightforwardly compute the phase profile $\dot{s}^\star(t)$ simply as $\dot{s}^\star(t) = \boldsymbol{\varphi}'(s(t))^{-1} \cdot \dot{\boldsymbol{\varphi}}^\star(t)$, as (3) ensures $\boldsymbol{\varphi}'(s)$ to be always defined. In Section 4.2 we show how this property can enhance human-robot cooperative tasks.

The operation of the spatial sampling algorithm is graphically shown in Fig. 1. The demonstrated trajectory $y(t)$ is first sampled with a sampling time T, in order to construct the linearly interpolating function $y_L(t)$ as in Fig. 1(a). Subsequently, in Fig. 1(b), the spatial sampling algorithm is applied to the curve $y_L(t)$ using a certain spatial interval δ, where it can be noticed that a more accurate approximation of the original curve can be achieved for smaller parameters δ. Fig. 1(a) shows that the proposed spatial sampling imposes no constraints on the demonstrated trajectory $\boldsymbol{y}(t)$, which can also include parts with zero speed which might occur if the user stops during the demonstration. This is an important feature since no segmentation of the demonstrated trajectory is required, as done by other approaches [2].

3 Control Architecture for Human-Robot Interaction

A novel control architecture, combining admittance control with guiding virtual fixtures, has been developed to constrain the motion of the robot's end-effector along a 3D path specified by the therapist, without enforcing a specific temporal profile [10, 12]. This approach allows the patient, connected to the robot's end-effector, to impose the movement along the curve by applying forces with the rehabilitated limb.

Let us consider the reference path defined in the previous section and denoted as $\boldsymbol{\varphi}(s)$, which has been recorded by the therapist through kinhestetic teaching. Thanks to the SSA, the function $\boldsymbol{\varphi}(s)$ is a regular curve, with $\boldsymbol{\varphi}'(s) = \mathrm{d}\boldsymbol{\varphi}(s)/\mathrm{d}s$ being always well-defined. In the experiments, the analytical expression of $\boldsymbol{\varphi}(s)$ was obtained as a sum of Bernstein basis functions [11]. As the current application aims to enforce a specified geometric path constrain, the arc-length parameterization is used, which is indeed directly provided by the SSA [12].

As depicted in Fig. 2, a point-wise mass m is constrained to follow the path $\boldsymbol{\varphi}(s)$, moving under the influence of the force applied by the user to the robot's end-effector. Simultaneously, the robot must accurately track the mass's position. The Admittance Guiding Virtual Fixture is implemented by computing the forward dynamics of the virtual mass, considering the measured force $\hat{F}_h$. This approach allows us to determine the instantaneous reference position $\boldsymbol{y}_d(t) = \boldsymbol{\varphi}(s(t))$. The dynamic model of the point mass m in Fig. 2 is derived by applying Lagrange's equations. Under the assumption that the mass constrained to the curve $\boldsymbol{\varphi}(s)$ is not affected by gravity, the Lagrangian function $\mathcal{L}$ equals the kinetic energy $\mathcal{K}$, that is:

$$\mathcal{L} = \mathcal{K} = \frac{1}{2} m \dot{\mathbf{y}}_d^T \dot{\mathbf{y}}_d = \frac{1}{2} m \dot{s}^2. \tag{4}$$

From (3) and observing that $\dot{\mathbf{y}}_d = \boldsymbol{\varphi}'(s)\dot{s}$, one can write 4 as

$$m\ddot{s} + b\dot{s} = F_{\parallel}, \tag{5}$$

where $b\dot{s}$ is a non-conservative term representing friction, and $F_{\parallel}$ is the component of the force $\hat{\boldsymbol{F}}_h$ applied by the user to the robot tool (detected by a force sensor) that is tangent to the curve, i.e.

$$F_{\parallel} = \boldsymbol{\varphi}'(s)^T \cdot \hat{\boldsymbol{F}}_h, \tag{6}$$

where, from (3), $\boldsymbol{\varphi}'(s)$ represents the unit tangent vector to $\boldsymbol{\varphi}(s)$ at a generic point s.

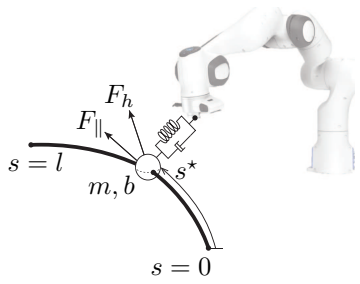

Figure 2: Working principle of the proposed control architecture based on a constrained point-wise mass

4 Experiments and Evaluation

4.1 Robot Handwriting Comparisons

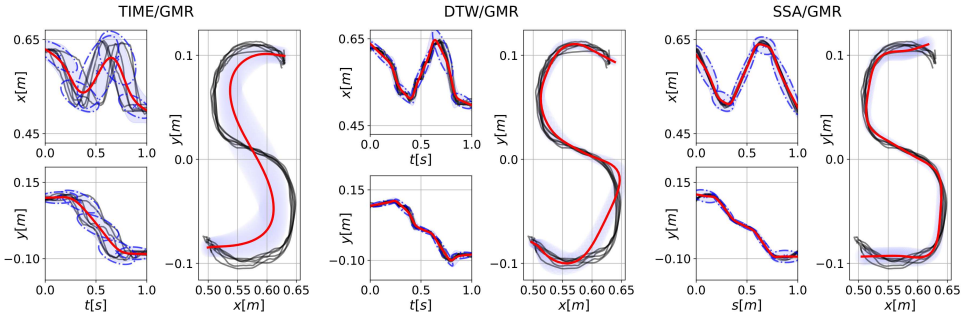

Figure 3: Comparison of barycenter computation.

This section aims to analyze the geometric approximation error when calculating the barycenter of a group of demonstrated trajectories. To achieve this, we analyzed end-effector position recordings, where users repeated the same geometric path six times for each symbol, varying speeds and introducing pauses [10, 11]. We tested three scenarios: (i)

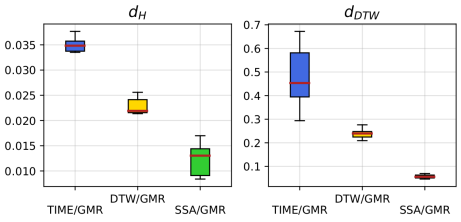

Figure 4: Haussdorff (d_H) and DTW (d_{DTW}) distance comparizons.

Table 1: Mean and standard deviation values for approximation metrics.

	$d_H\,(e^{-2})$	$d_{DTW}\,(e^{-1})$
TIME/GMR	3.5±0.15	4.8±1.25
DTW/GMR	2.3±0.16	2.4±0.22
SSA/GMR	**2.0±0.36**	**0.8±0.12**

feeding time-based recordings to GMR (TIME/GMR), (ii) using DTW to align trajectories before applying GMR (DTW/GMR) (iii) filtering recordings with SSA before sending them to GMR (SSA/GMR). GMR is widely used in robotics for skill extraction, which justifies its inclusion in this study [8]. Additionally, the DTW/GMR combination has been adopted in many seminal robotics works, making it a relevant comparison algorithm [4, 9].

The error between recorded trajectories and their respective barycenter was defined in terms of Haussdorff (d_H) and, without loss of consistency, DTW (d_{DTW}) distance. Figure 3 plots the results for S-shape recordings. Before using GMR to compute the barycenter (red), we fit a GMM to the demonstrated trajectories (black) with $N = 5$ components (blue). At a first look one can observe that in Fig. 3a temporal distortions leed to high variance demonstration, thus lowering the quality of the retrieved skill. Substantial lower variances are obtained for the DTW/GMR and SSA/GMR case (Fig. 3b and 3c), the former exhibiting a qualitative whorse shape for the barycenter, which may depends on the choice of the reference to align the trajectories. Quantitative values are provided in Fig. 4 and Table 1, where one can clearly see how the proposed SSA/GMR combination outperforms the others. Indeed, unlike the common DTW/GMR approach where trajectory alignment is required and performed using DTW, our SSA filters the trajectories to obtain their arc-length counterpart, thus filtering out time distortions. Similar results were observed when applying this approach to other trajectories, such as those from the Panda Co-Manipulation Dataset introduced in [13].

Moreover, one can underline two important aspects. The first one is that intuitively by increasing the number of Gaussian N better results can be achieved, particularly in the DTW/GMR and SSA/GMR cases. However, as shown in [13], the quality of the skill extrapolated in the DTW/GMR case can still be affected by the reference alignment trajectory. This is not the case for SSA, which does not require a reference.
Second, while spatial consistency across demonstrations is essential, timing variations introduce noise, potentially degrading the GMM model's quality (see Fig.3-4). We demonstrated that using SSA to capture only the geometric path improves skill representation by filtering out timing inconsistencies, leading to better skill learning.

4.2 Rehabilitation Task

The rehabilitation process benefits significantly from a learning-by-demonstration procedure, where the therapist can freely demonstrate and teach the exercise to the robot. This approach allows the therapist to directly guide the robot, effectively transferring their knowledge of the task to the system. By doing so, the therapist shapes the rehabilitation exercise, enabling the patient to reproduce it more naturally and accurately. The proposed method simplifies following the demonstrated path, enhancing the overall effectiveness and personalization of the rehabilitation session.

The rehabilitation tests involved a straightforward exercise aimed at assessing the patient's ability to extend and flex the arm. This task validated the effectiveness of the developed framework, enabling the patient to successfully carry out the required movements. Specifi-

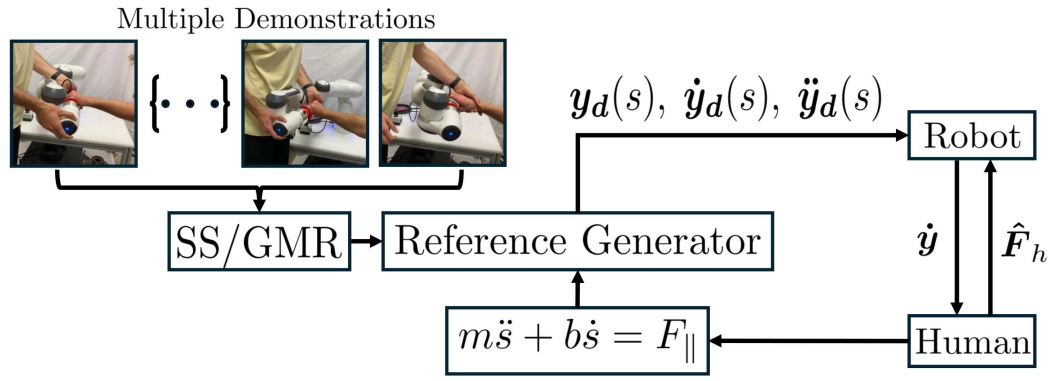

Figure 5: Schematic of the proposed architecture.

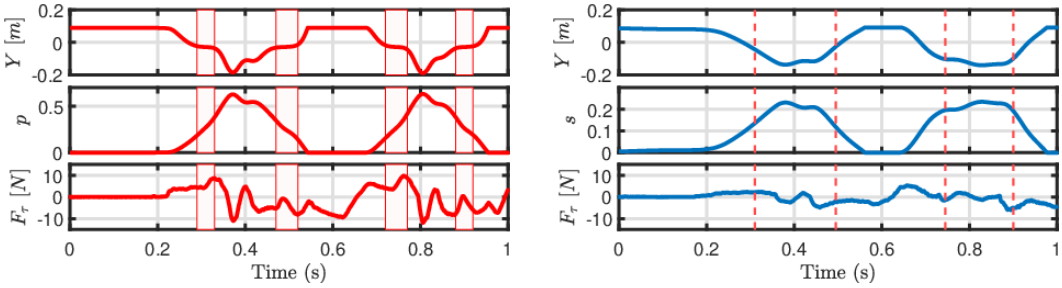

(a) (b)

Figure 6: Comparison of results: (a) Traditional method without Spatial Sampling, and (b) Proposed method with Spatial Sampling.

cally, the advantages of the SSA were highlighted by comparing it to a traditional solution based on phase variable control. A schematic of the proposed architecture is illustrated in Fig. 2.

The traditional approach, which relies on variations in a phase variable, often results in stagnation. This phenomenon is related to the velocity imposed during task execution, described analytically as:

$$\dot{\boldsymbol{y}}_{\boldsymbol{d}}(p(t)) = \frac{d\boldsymbol{\varphi}(p(t))}{dp}\dot{p}$$

As highlighted by red intervals in Fig. 6a, the patient may continue to exert forces, altering the phase variable p and modulating its time derivative $\dot{p}$. However, the position along the constraint remains unchanged because multiple values of p can correspond to the same point on the path the patient is meant to follow. This type of mapping happens every time pausing intervals are present in the demonstration trajectories. As a consequence, the term $\frac{d\boldsymbol{\varphi}(p(t))}{dp}$ approaches zero, leading to a zero velocity during task execution and generating the stagnation phenomenon.

This limitation is overcome with the proposed framework in Fig. 6b. In this case, the change in position along the reference can be defined as:

$$\dot{\boldsymbol{y}}_{\boldsymbol{d}}(s(t)) = \frac{d\boldsymbol{\varphi}(s(t))}{ds}\dot{s},$$

where s is the arc-length parameter. One can clearly see that the phase evolution described by (5) never result in stagnation for the same position where the phenomenon happens in the first scenario. This result comes from the fact that, as shown in Section 2.1, applying SSA to the demonstrated trajectories produces regular curves with well-defined derivatives.

Consequently, the term $\frac{d\boldsymbol{\varphi}(s(t))}{ds}$ remains non-zero, as described in (5). This approach prevents stagnation and promotes smoother human cooperation, reducing the force required by the patient and enhancing the natural performance of the task.

5 Conclusion

In this paper we introduced a novel technique, the Spatial Sampling algorithm (SSA), which processes time-based Euclidean trajectories to extract their geometric paths, parameterized by the arc-length parameter. The SSA filters the input trajectory, producing evenly spaced samples along the path, and providing a regular curve with well-defined derivatives. We demonstrate how SSA offers a robust alternative to traditional alignment methods like DTW, particularly in Learning by Demonstration (LbD) scenarios. By removing time information, which can introduce distortions, SSA ensures more accurate skill representation.

The arc-length parametrization supports applying any timing law to the constrain curve. We utilized this to design a phase-update law suited for upper-limb rehabilitation tasks, enabling the robot to impose virtual constraints while allowing the user to navigate along the guide using force feedback applied to the end-effector. This phase-update law includes adjustable knot parameters to modify the execution style, enhancing exercise flexibility. In this context, multiple demonstrations could be provided to define the target task, each one characterized by its own timing and possibly including pausing intervals. In the experiments we showed how applying the SSA could facilitate the learning of a constrain curve which enhances a more natural execution of the exercise, and avoids the problem of stagnation due to the presence of pausing intervals.

References

[1] P. Pastor, H. Hoffmann, T. Asfour, and S. Schaal. Learning and generalization of motor skills by learning from demonstration. In *2009 IEEE International Conference on Robotics and Automation*, pages 763–768. IEEE, 2009.

[2] T. Gašpar, B. Nemec, J. Morimoto, and A. Ude. Skill learning and action recognition by arc-length dynamic movement primitives. *Robotics and autonomous systems*, 100: 225–235, 2018.

[3] C. G. L. Bianco and F. Ghilardelli. A scaling algorithm for the generation of jerk-limited trajectories in the operational space. *Robotics and Computer-Integrated Manufacturing*, 44:284–295, 2017.

[4] H. Su, A. Mariani, S. E. Ovur, A. Menciassi, G. Ferrigno, and E. De Momi. Toward teaching by demonstration for robot-assisted minimally invasive surgery. *IEEE Transactions on Automation Science and Engineering*, 18(2):484–494, 2021.

[5] M. Müller. Dynamic time warping. *Information retrieval for music and motion*, pages 69–84, 2007.

[6] P. Senin. Dynamic time warping algorithm review. *Information and Computer Science Department University of Hawaii at Manoa Honolulu, USA*, 855(1-23):40, 2008.

[7] F. Petitjean, A. Ketterlin, and P. Gancarski. A global averaging method for dynamic time warping, with applications to clustering. *Pattern recognition*, 44(3):678–693, 2011.

[8] S. Calinon, F. Guenter, and A. Billard. On learning, representing, and generalizing a task in a humanoid robot. *IEEE Transactions on Systems, Man, and Cybernetics, Part B (Cybernetics)*, 37(2):286–298, 2007.

[9] J. Zheng, Z. Li, L. Huang, Y. Gao, B. Wang, M. Peng, and Y. Wang. A gmm-dtw-based locomotion mode recognition method in lower limb exoskeleton. *IEEE Sensors Journal*, 22(20):19556–19566, 2022.

[10] G. Braglia, D. Tebaldi, and L. Biagiotti. Phase-free dynamic movement primitives applied to kinesthetic guidance in robotic co-manipulation tasks. *arXiv:2401.08238*, 2024.

[11] G. Braglia, S. Calinon, and L. Biagiotti. A minimum-jerk approach to handle singularities in virtual fixtures. *IEEE Robotics and Automation Letters*, pages 1–8, 2024. doi:10.1109/LRA.2024.3469814.

[12] D. Onfiani, M. Caramaschi, L. Biagiotti, and F. Pini. Path-constrained admittance control of human-robot interaction for upper limb rehabilitation. In F. Cavallo, J.-J. Cabibihan, L. Fiorini, A. Sorrentino, H. He, X. Liu, Y. Matsumoto, and S. S. Ge, editors, *Social Robotics*, pages 143–153, Cham, 2022. Springer Nature Switzerland. ISBN 978-3-031-24667-8.

[13] G. Braglia, D. Tebaldi, A. E. Lazzaretti, and L. Biagiotti. Arc-length-based warping for robot skill synthesis from multiple demonstrations. *arXiv preprint arXiv:2410.13322*, 2024.